THE EFFECTS OF FABRICATION PROCESSES ON I_{sc} AND V_{oc} OF MONOCRYSTALLINE SILICON SOLAR CELL CHARACTERISTICS

By

MOTAHHER ABDALLAH HASSAN QA'EED

Thesis Submitted in Fulfillment of the Requirements

For the Degree of

Master of Science

UNIVERSITY SAINS MALAYSIA

2011

ACKNOWLEDGMENTS

First of all, I would like to thank Allah for giving me the strength and perseverance while doing my research. Secondly, I would like to express my appreciation to my supervisor, Professor Dr. Hajj. Kamarulazizi bin Ibrahim for his guidance and comments on my research. His encouragement, advice, and kindness seriously put me in the right direction to be a researcher. I am honored to be one of his students.

I would like to thank the current Dean Professor Zainuriah Abu Hassan and the previous Dean of School of Physics, Professor Haslan Abu Hassan.

I would like to thank the professional editor, Mr. Ghayth al-Shaibani for his voluable comments and editing. I would like to extent my appreciation to all my friends who encouraged me during this work: Osama Saad Hammad, Omer Mahfoodh, and Abdalhameed al-Namshah.

I would like to thank all the technicians at the School of Physics for their help during my work in the laboratory and Universiti Sains Malaysia which gave me the chance to pursue my M.Sc at the School of Physics where I have had ample access to various facilities and attended various colloquiums and workshops.

Many thanks go to Hodeidah University for the financial support it offered me to pursue my M.Sc at Universiti Sains Malaysia.

I would like to thank my parents and all the members of my family for their patience being away from them. Their prayers have helped me a lot during my research.

TABLE OF CONTENTS

LIST OF TABLES

LIST OF FIGURES

LIST OF ABBREVIATIONS

Abbreviation	Meaning
BSF	Back surface field
RTP	Rapid thermal process
RIE	Reaction ion etching
PECVD	Plasma Enhanced Chemical Vapor Deposition
UV	ultraviolet
IPA	Isopropyl alcohol
ARC	Anti-reflection coating
Cz	An abbreviation for a single crystal grown by the Czochralski method.
NOR	Nanotechnology optical research
ESI	Edge shunt isolation

LIST OF SYMBOLS

Symbol	Meaning
r	Resistivity
D	Diffusion coefficient
I_{sc}	Short circuit current
V_{oc}	Open circuit voltage
ϕ	The electric potential
ε	The materials permittivity
ε_o	The permittivity of the space
dE	Electric field gradient
$d\chi$	Length space charge gradient
N	Densities of electrons
P	Densities of holes
N_D^+	Density of donors
N_A^-	Density of acceptors
I_p	Holes current density
I_n	Electrons current density
μ_n	Mobility of electrons
μ_p	Mobility of holes
D_n	Electron diffusion coefficient
D_p	Holes diffusion coefficient
K	Boltzman coefficient
T	Temperature in Kelvin

Q	Electron charge
U	Recombination rate of the carriers
G	Carrier's generation rate
N_c	The effective density of states in the conduction band
N_v	The effective density of states in the valence band
E_F	Energy of Fermi level
E_c	Conduction band
Ev	Valence band
v_D	Potential built in
E	Exponential constant
n_n	The majority carrier in n-type
p_p	The majority carrier in p-type
p_n	The minority carrier in n-type
n_p	The minority carrier in p-type
n_i	Intrinsic carrier concentration
Na	The concentration of acceptor
Nd	The concentration of donor
I_{recomb}	Recombination current
I_{gd}	Generation current of electron
$I_o = I_{OE}$	Dark saturation current
$I_{gl} = I_L$	The photogenerated electron current
V_{mp}	The voltage at the maximum power point
I_{mp}	The current at the maximum power point
FF	The fill factor
η	The efficiency of the cell

P_{in}	The incident illumination power
A^{o}	Angstrom
J	Flux of the donor or acceptor impurities types
t	Time
N_{o}	Impurity concentration at the wafer surface
$N_{(x,t)}$	Impurity concentration at distance x from the surface during t minutes
erfc	Complimentary error function
Q	The total number of impurity atoms per unit area in the silicon
E_{A}	Active energy
χ_{i}	Diffusion depth
N_{B}	Background concentration
N	Reflective index
D	Layer thickness
λ	Wavelength
R	Reflection factor
T	Lifetime
n_{o}	The reflective index of the uppermost layer
n_{1}	The reflective index of the anti-reflection layer
n_{2}	The reflective index of the silicon
$q\varphi_{m}$	A metal work function
$q\varphi_{s}$	Semiconductor work function
$q\chi$	Electron affinity
V_{o}	The equilibrium potential deferent
I_{E}	Stands recombination current of the edge,
UV	Ultraviolet

IPA	Isopropyl alcohol
BSF	Back surface field
Al	Aluminum
ρ	Resistivity
s	Conductivity
B_z	Magnetic field
R_H	Hall resistance

Kesan Proses Fabrikasi ke Atas Ciri- Ciri I_{lp} dan V_{lt} Sel Suria Silikon Hablur Tunggal

ABSTRAK

Tesis ini menumpukan kepada fabrikasi sel suria di dalam makmal NOR dengan menggunakan sumber resapan fosforus dan boron serta mengukur kesan proses-proses fabrikasi terhadap sel suria silikon hablur tunggal. Untuk menjalankan kajian ini, pengkaji menggunakan beberapa teori dan persamaan yang bersesuaian.

Proses-proses yang telah dijalankan dalam kajian ini adalah penipisan wafer, pemancaran boron bagi meningkatkan medan permukaan belakang (MPB), pentekstur permukaan, pemancaran fosforus bagi menghasilkan emitter, rawatan haba, salutan lapisan anti-pantulan, pengasingan hujung pirau dan pelogaman. Larutan KOH memainkan peranan dalam pentekstur permukaan. Larutan berasid memainkan peranan dalam penipisan wafer.

Proses-proses ini diukur dengan menggunakan pengukuran I_{lp} arus litar tertutup dan V_{lt} voltan litar terbuka yang mudah dan terus. I_{lp} arus litar tertutup dan V_{lt} voltan litar terbuka dikira sebelum dan selepas atau dengan/tanpa setiap proses, selain penipisan wafer dan proses-proses (BSF) termasuk dua kumpulan sampel, yang mana kumpulan pertama diukur dengan menerapkan proses. Sedangkan untuk kumpulan kedua diukur tidak menerapkan proses. Pengukuran elektrik ini digunakan sebagai faktor utama dalam kajian ini untuk menunjukkan kecekapan sel suria. Kaedah pengukuran ini memendekkan masa langkah pencirian di dalam makmal.

Dalam kerja ini, nilai purata V_{lt} bagi wafer yang tebal adalah 345 mV dan 415 mV bagi wafer yang nipis (< 200 μm tebal). Manakala, purata nilai I_{lp} bagi yang tebal adalah 6.15 mA dan 8.05 mA bagi sel suria yang nipis. Purata nilai V_{lt} dengan

MPB adalah 163mV, dan 360 mV tanpa MPB. Sebelum proses pelogaman, nilai purata V_{lt} adalah 350mV. Walau bagaimanapun, ia menjadi 398 mV selepas proses pelogaman. Sebelum pelogaman, nilai purata I_{lp} adalah 5.25 mA dan 8.13 mA selepas proses pelogaman. Dalam kajian ini, nilai purata V_{lt} sebelum proses pengasingan pirau adalah 412 mV. Ia menjadi 426 mV selepas proses pengasingan pirau. Manakala, nilai purata I_{lp} bertambah dari 8.9mA kepada 9.7mA disebabkan proses pengasingan pirau. Kedalaman resapan fosforus dalam sel suria hablur tunggal χ_j adalah 2.457 μm Kecekapan sel suria untuk keadaan yang optima adalah 9.51% dan faktor isi (FF) adalah 0.79. Kerja ini menghasilkan gambaran yang jelas tentang ciri-ciri elektrik dalam setiap proses secara berasingan.

The Effects of Fabrication Processes on I_{sc} and V_{oc} of Monocrystalline Silicon Solar Cell Characteristics

ABSTRACT

This thesis is concerned with the fabrication of a solar cell in NOR laboratory using phosphorus and boron diffusions to measure the effect of the fabrication processes on the monocrystalline silicon solar cell. To carry out this, the researcher has employed a number of relevant theoretical concepts and equations.

The processes which were performed included thinning the wafer, diffusing the boron to improve the back surface field (BSF), texturing the surface, diffusing phosphorus to create the emitter, annealing, anti-reflection coating, metallization, and edge shunt isolation. KOH solution was used and it played the role of texturing the surface. Acidic solution was used and it played the role of thinning the wafer.

These processes were measured by easy and direct measurements of short circuit current (I_{sc}) and open circuit current (V_{oc}). The short circuit current and open circuit voltage were measured before and after each process, except for thinning the wafer and (BSF) processes which include two groups of samples the first group is measured with applying the process. The second group was measured without applying the process. These electrical measurements were used as the main factors in this study to examine the solar cell's output. The method of measurement shortens the measurement time of characterization steps in the laboratory.

In this work, the average of V_{oc} was 345 mV and 415 mV for the thick and thin (< 200 μm thick) solar cell respectively; while, the average of I_{sc} for the thick and thin solar cell was 6.15 mA and 8.05 mA respectively. The average V_{oc} with and without apply BSF were 163 mV and 360 mV, respectively. Before the metallization

process, the average of V_{oc} was 350 mV. However, it became 398 mV after the metallization process. The average of I_{sc} was 5.25 mA and 8.13mA before and after the metallization process, respectively. In this research, the average of V_{oc} before and after the shunt isolation process was 412mV and 426 mV, respectively. While, the average value of I_{sc} increased from 8.9 mA to 9.7 mA due to the shunt isolation process. The phosphorus diffusion depth in monocrystalline silicon solar cell χ_j was 2.457μm. The solar cell efficiency under optimal conditions was 9.51% and the fill factor (FF) was 0.79. This work resulted in drawing a clear picture of the electrical characteristics in each process independently.

CHAPTER 1

INTRODUCTION

1.0 Introduction

Crystalline silicon is the most widely used material in the production of solar cells. It is the naturally an abundant element, has well-suited band-gap for solar cell conversion efficiency, and is a non-toxic. Furthermore, it is widely used in the microelectronics industry; it has become the most studied semiconductors (Green, 2001). On the other hand, the silicon solar cell is a very important device as it directly converts energy from sunlight into electricity without power consumption. Therefore, the electrical current derived from the solar cell has been known for decades and it has widely been acknowledged that it cannot be implemented as a primary energy source in industrialized countries.

In 1974, COMSAT laboratories improved the solar cells performance through the employment of surface texturing technique and back surface field formation (Haynos *et al.,* 1974). Random pyramids texturing was developed in microelectronics and then applied to solar cells fabrication by COMSAT laboratories. They reduced reflection loss. Back surface field (BSF) was developed at NASA Lewis Research Center by driving the impurities towards the backside of a p-type wafer (Mandelkorn & Lamneck, 1972). The degree of impurity concentration (p − p+) results in repelling the electrons generated in the base region towards the front junction. Multi-crystalline silicon material involves relatively simpler and cheaper crystal growth technologies such as float zone (FZ) and Czochralski (Cz silicon) than the mono-crystalline Silicon. The mono-crystalline silicon material, which is the focus of this research, can be of low cost by thinning the wafer involved with wafer

slicing (Nakayashiki *et al.*, 2005). However, the output of the solar cells can be developed through manufacturing processes in the laboratory.

1.1 Statement of the problem

The development of an efficient solar cell has already been done by a number of researchers in this area. For example, Ruby *et al.* (1999) and Damini *et al*. (2000) and others studied texturing. Nostell (2000) and Qingna *et al.* (2007) and others studied the antireflection coating. Li Cai and Ajeet Rohatgi (1997) studied the effect of annealing. Zhao *et al.* (1996) studied the metallization. Al Rifai *et al.*(2003) worked on edge shunt isolation. Other fabrication processes of the solar cell have been done in order to improve the output. However, these studies were carried out under very different conditions. For example, in these studies, the processes were achieved under different laboratories, different types of dopant used in the diffusion, different diffusion temperature, and different tools of measurement. The researcher believes that to develop a solar cell, one needs to know the most effective process(es) on the output of solar cell. This will help work on only the most effective process(es) to better improve the efficiency in the future studies.

This research is devoted to study the characteristics of each manufacturing processes independently under the same conditions in the laboratory because they have not been measured independently under the same condition in the previous studies. The purpose is to find out how each process affects the power generated in the solar cells. This will help conduct another study where the process, which results in the most effective output of the solar cells, will be focused on in the future research. These processes could be developed by further research.

Many researchers such as Macdonald *et al*. (2001) and Gangopadhyay *et al.* (2005) have proved that texturing is very important and it plays an effective role in increasing the output of a solar cell. Hence, there is a need to find out the most effective characteristics of the surface on the output of the solar cell.

This study will use a new type of dopant (a solid diffusion source of phosphorus). This type will be used for the first time in NOR laboratory to fabricate a solar cell. It is known that different parameters affect the diffusion process. These parameters include diffusion temperature, the flow of N_2 gas, and diffusion time. These parameters must be taken into account in this study because they change under different conditions such as tube furnace, dopant type, and type of gas .

1.2 Scope of study

In this study, the dopant phosphorus parameters will be studied under the same conditions to choose the best parameters' values of the N_2 gas flow, temperature, and time of diffusion. Then, these best values will be used in all the processes involved in this study.

The researcher will then make a comparison between the two types of texturing on the front surface of the cell to one flat surface to know the characteristics of each type if it is effective in raising the output results.

In the present study, solar cells will be fabricated using mono-crystalline silicon wafer. Fabrication processes such as thinning the wafer, back surface field, texturing on the front surface, annealing, anti-reflection coating, metallization and shunt isolation will be investigated. Solid-source diffusion will be used to fabricate the emitter.

The researcher would like to introduce a simpler measurement technique. This technique of measurements will be taken by a voltmeter and current meter in the direct measurement of the short circuit current (I_{sc}) and open circuit voltage (V_{oc}) during each process. The short circuit current and open circuit voltages will be employed in this work because they are considered the most important parameters in the solar cell and because their multiplication gives an indication of output energy in the solar cell. This method of measurement is simple, direct and it shortens the measurement time of characterization steps in the laboratory.

1.3 Research objectives

In light of the above, the present study has the following objectives:

1- To fabricate and study each process independently of mono-crystalline silicon wafer of solar cell.

2- To study the effects of texturing on $\mathbf{I_{sc}}$ and $\mathbf{V_{oc}}$.

3- To use solid source diffusion (such as Boron and Phosphorus) and to measure the doping concentration and junction depth of the emitter.

1.4 Thesis organization

In Chapter 1, the subject of the study is introduced which includes the monocrystalline silicon significance, the justification of the study, a new measurement method, and the objectives of this study. **Chapter 2** presents a comprehensive literature review on phosphorus diffusion, boron diffusion, texturing, annealing, anti-reflection coating, and shunt isolation. **Chapter 3** gives a detailed explanation of the physics of solar cell. The theories of p-n junction of the solar cell, phosphorus diffusion, oxidation, trapping the light (anti-reflection coating and texturing), the theoretical equations of the output measurement of the solar cell, are

also discussed in this part of the thesis. In **Chapter 4**, various methods of the fabrication processes are presented and explained in detail. All the solar cell fabrication processes are carried out in the NOR laboratory in the School of Physics, at Universiti Sains Malaysia. **Chapter 5** provides explanations and analyses of various results of the solid diffusion source and effects of fabrication processes on I_{sc} and V_{oc}. **Chapter 6** including the conclusion of this study, which achieve the study objectives, followed by some recommendations and suggestions for future research.

CHAPTER 2

LITERATURE REVIEW

2.0 Introduction

In this chapter, a brief review of the phosphorus (p) used to produce emitter diffusion in Si solar cells is presented. Texturing the front surface, anti-reflection coating and how boron (b) is used to produce back surface field (BSF) in the solar cell are also discussed in this chapter.

2.1 Dopant diffusion

The physics and applications of diffusion in Si have received serious interest over several decades, primarily due to the great technological importance of dopant diffusion in fabricating microelectronic devices. However, the diffusion of impurities in the silicon constitutes many processes which a silicon wafer undergoes to yield a solar cell. Phosphorus and boron are the two most commonly used impurities to form an emitter and base regions of the solar cells, transistors and integrated circuits. Basically, diffusion involves heating the silicon wafer to a temperature at which the diffusion coefficient of the impurity is reasonably large whereby the vapor of the impurities is allowed to pass through the diluted carrier gas over the entire silicon surface to form the active region. The phosphorus and boron own high solubility in silicon and this makes them potential elements to be used in solar cell fabrication and other devices. Therefore, the phosphorus diffusion and boron diffusion are discussed in the sub-sections below.

2.1.1 Phosphorus diffusion

While processing the solar cell on the p-type silicon substrate, the emitter is usually created by the diffusion from the phosphorus source to the sample surface. There are various methods used to form such phosphorus diffused emitters when the phosphorus is deposited from the source to the silicon, for example (from a gaseous liquid, or solid diffusion source of sufficiently high concentration). Diffusion profiles differ considerably from Gaussian or complementary error function distributions which are regularly observed (Tannenbaum, 1961; Tsai, 1969). In particular, Tannenbaum reported that when the concentration near the surface is sufficiently high (which frequently occurs in the solar cell emitters), an essentially flat plateau near the surface will be exhibited (Tannenbaum, 1961).

Furthermore, for high phosphorus concentration in-diffusion in the Si, diffusion profiles that consist of the characteristic kink-and-tail shape are frequently obtained (Lee & Willoughby, 1972). Because of this, the kink-and-tail profiles are often described is due to a dual diffusion mechanism. Larsen *et al*. (1983) used diffusion temperature between (1000-1200)$^{\circ}$C when they doped silicon single crystal with arsenic or phosphorus in silicon wafers (100) and (111).

Mouhoub *et al*. (2003) used screen printing and belt furnace at 980°C. They used two methods: selective emitters of deeply diffused regions with a high surface concentration and shallow emitter region at a low surface concentration. The two methods enhanced current; for the first one, the current was 1.5 and for the second method, the current was 1.3 mA /cm^{2}. However, in 2005 Basu used $POCl_3$ diffusion at 850°C within deposition time range 5-15 minutes. Thereafter, oxides at 850°C were used drive in for 15 minutes in his work on a Low-Cost technique of emitter-

junction optimization in monocrystalline silicon solar cells with an area of 12.5x12.5 cm^2.

During the analysis of the phosphorus doped emitter profiles of multicrystalline silicon solar cells, Brammer *et al*. (2001) used $POCl_3$ between (800-900)°C in tube furnace to produce emitter diffusion. Kittidachachan *et al.* (2007) formed an emitter layer on the front surface of solar cells using phosphorus diffusion.

They used solid diffusion source at 1000°C for 30 minutes, and then they applied various processes to optimize the solar cell I_{sc} and V_{oc} simultaneously. The high short circuit current density used was 15.94mA/cm^2**;** while the high open circuit voltage was 564.8mV which is shown in figure 2.1.

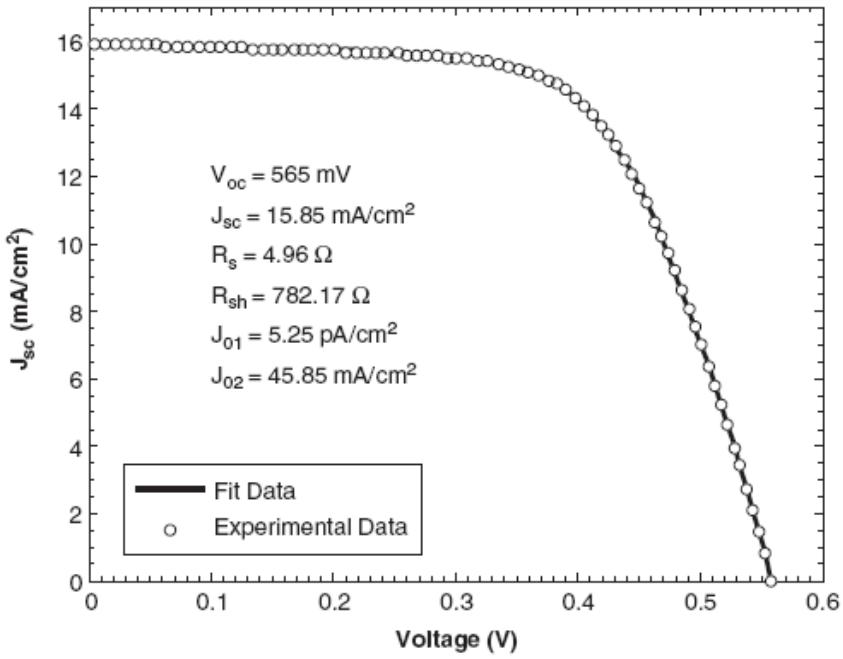

Figure 2.1: I–V characteristics of the solar cell [adapted from Kittidachachan *et al*., (2007)]

However, in the present study, the solid diffusion source will be used with the optimal values of temperature, time, and flow rate of nitrogen gas.

2.1.2 Boron diffusion

The application of boron diffusion to form the emitter in silicon solar cells processing has received little attention over the last 20 years. Boron diffusion has been characterized by a variety of techniques. Some relied on the open circuit voltage and fill factor of a completed solar cell (Ebong 1994). Other researchers took fundamental approaches by measuring the emitter saturation current (Kane & Swanson, 1985; King *et al.*, 1990; Cuevas *et al.*, 1997; Krygowski *et al.*, 1997). There are also reports on the lifetime of the impurities and diffusion length to test the solar cell structure (Fossum & Burgess, 1978; Wang *et al.*, 1990). which had received boron diffusion over the entire surface. However, the demonstration of similar emitter saturation current for phosphorus and boron diffusions was first presented by Kane and Swanson (1985). These researchers used pre-deposition and drive in. they used doped chemical vapour deposition (CVD) SiO_2 at ~ 400°C and driven in at temperature over 1000°C.

2.2 Back surface field (BSF)

For an effective back surface field (BSF), the doping of the back layer should be high (over 10^{17} cm^{-3}) and the depth of the BSF should be in the order of several microns. Boron has the potential to provide an improved BSF compared with an Al/Si alloy as the density of the boron's atoms can be higher than the Al doping in an Al/Si alloy. Aluminum back surface field can increase the efficiency of poly crystalline silicon solar cells by about 10% (Koval *et al.*, 1996). This increase is due to the increase in the optical reflections from the aluminum on the rear surface. Aluminum back surface field also decreases the surface recombination velocity. Accordingly, the minority carrier diffusion length increases in the base of the solar cell (Koval *et al.*,

1996). In the industry, aluminum paste is used to develop the solar cell by building the back surface field and thinning the wafer which shows good electrical characteristics (Khadilkar *et al.*, 2005).

Boron deposition methods vary and depend on the amount of the boron incorporated into the silicon. Boron diffusion is used to build the BSF, resulting in high lifetime of carriers in the bulk. This occurs when it is properly done with dielectric passivation used for boron diffusion through drive in and rapid thermal process. However, in this case, the contamination and defects resulted from diffusing the boron into the wafer. For this reason, the value of V_{oc} was less than 600 mV (Lee, 2004).

Solid diffusion source has a higher dose than the one can be obtained by a BBr_3 source of diffusion to the silicon if a high temperature of the solid diffusion source is not used. Furthermore, the solid source diffusion of boron varies in its concentration through the gas flow and deposition temperature. This diffusion can be optimized with time by simply increasing the deposition temperature. This means that deposition can be optimized by increasing in the temperature and/or changing the time and the gas flow. However, in this study, boron diffusion will be deposited on the back surface of the wafer. It is expected that this method can achieve the characteristics of the back surface field as it will be discussed in details in Chapter Five.

2.3 Texturing the font surface

Damini *et al.* (2000) used reactive ion etching with a maskless plasma texturing technique in silicon solar cells which resulted in a very low reflectance of 5.4 % before depositing SiN and 3.9 % after depositing SiN.

In industrial multicrystalline silicon solar cells, there are many techniques of texturing processes used previously. Some have focused on using RIE with a mask to

achieve large and regular features (Winderbaum *et al.*, 1997), or without a mask to achieve random texture (Ruby *et al*., 1999). Others used isotropic wet acidic etching (Wolf *et al.*, 2000). However, Macdonald *et al*. (2001) found that wet acidic texturing, masked reaction ion etching (RIE) and maskless RIE all significantly reduce reflection losses in the solar cells. The reduction in reflection was greater with the masked RIE pyramids, followed by maskless RIE and acidic texturing (Macdonald *et al.*, 2001).

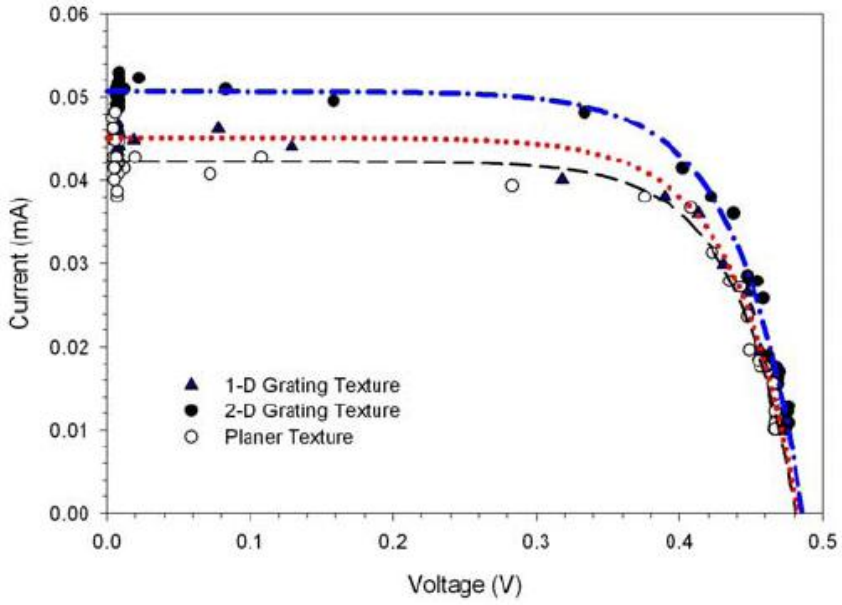

Figure 2.2: I-V plot of a 2D textured solar cell with and without anti-reflection nitride layer of 2cm^2 under 1kWatt/m^{2}measurement [adapted from Jahanshah *et al*., (2007)]

Sodium hydroxide and/or sodium hypochlorite was used for texturing and resulted in a textured surface with regular pyramids. This process increased open circuit voltage and short circuit current. Jahanshah *et al.* (2007) used grating to successfully make better texturing. Sparber (2003) studied two aqueous solutions of surface texturing. The first solution consisted of Potassium hydroxide (KOH) and isopropyl alcohol (IPA). The second one was sodium carbonate (Na_2CO_3)/$NaHCO_3$. Subsequently, the results obtained indicated that the reflection depends on etching time, solution

temperature and solution concentration. Therefore, the increase in the amount of Na_2CO_3 results in an increase in the density of the pyramids; while, the formed hills form disappear. But the formation process of the pyramids in Na_2CO_3/$NaHCO_3$ solutions occurs in a different way than in KOH/IPA solutions. The pyramids formed through KOH /IPA grow and are distributed in a homogeneous manner on the whole surface of the silicon wafer. In Na_2CO_3/$NaHCO_3$ solutions, the pyramids growth starts after 15 minutes and the pyramids density is very high and where the temperature varied between 90-97°C (Sparber *et al.*, 2003). However, in the present study, at 90°C, for 25 minutes, and 35% of KOH solution will be used to make the texturing on the surface with different masks to study the differences in texturing characteristics.

Gangopadhyay *et al*. (2005) made a comparison between two different solutions used for texturing surfaces using NaOH–NaOCl and NaOH (40%) as solutions. The results are shown in Figures (2.3).

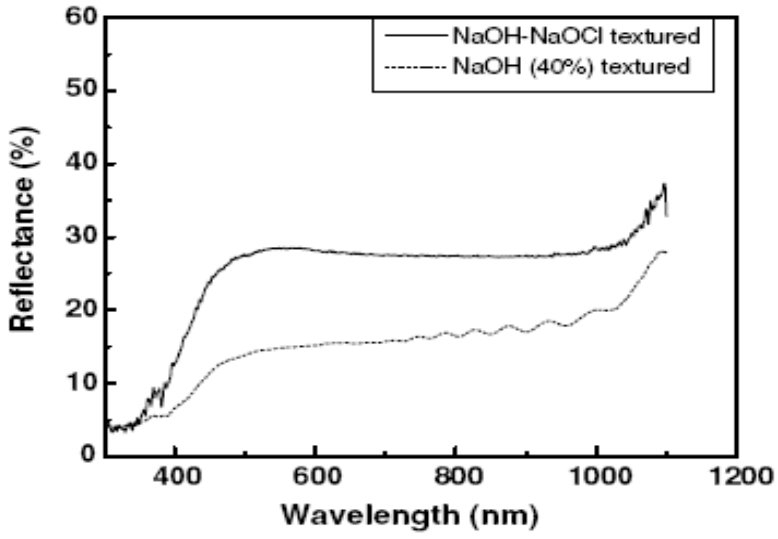

Figure 2.3: The reflections of different surfaces textured with NaOH-NaOCl and NaOH solutions [adapted from Gangopadhyay *et al*., (2005)]

2.4 Anti-reflection coating (ARC)

The first ever anti-reflection coating (ARC) was presumably made by Fraunhofer in 1817 who used sulphuric and nitric acid vapor to etch a glass. As a result of this etching, he noticed that the reflection greatly decreased. The decrease in the transmission of a transparent optical medium is caused by the abrupt change in the refractive index at the interface between the layer medium and its environment.

Taylor (1896) further developed this chemical etching process to form tarnished films which are now called anti-reflection coatings. A modern optical system (telescope, microscope or binoculars) would not work without ARC and the image would become blur due to the reflections in the various lenses (Nostell, 2000).

Anti-reflection coatings can range from a single layer to many layers where a single layer reflects only one wavelength over a wide spectral range. AR coatings have many applications in such as lasers, eye glasses, lenses, solar cells, IR diodes and spectral filters. Anti-reflection coating prevents a wavelength of the spectral range from getting reflected inside the layer; it also allows one wavelength to go through the layer and reflect. This is depends on the layer thickness (Asghar *et al.*, 2005).

The solar cell operates at a range of wavelengths from 300 – 1200 nm. This means that it needs a broadband ARC. In industry, a multi-crystalline silicon solar cell is manufactured by a single layer ARC which decreases the reflection dramatically compared to a bare silicon surface. Cid *et al*. (1998) found layers SiO_2/SiN structure had higher absorption at shorter wavelengths than a MgF_2/ZnS structure.

Plasma Enhanced Chemical Vapor Deposition (PECVD) has been known for many years to be one of the key technologies used for depositing the passivating Si_3N_4 anti-reflection coating. First of all, PECVD is generally regarded as a low–cost processing technique because the output rates are high and large areas can be deposited

during a process cycle. PECVD deposition can be carried out within a temperature range from room temperature up to over 500°C.

Furthermore, Indium-tin oxides (ITO) are the most widely used oxides for flat panel displays. This is because they have high optical transmittance in the visible region, high electrical conductivity, surface uniformity and process compatibility. It is possible to prepare ITO films using many techniques: spray pyrolysis, DC Sputtering, electron beam, and chemical vapour deposition. One general feature of plasma assisted deposition techniques compared to the thermal processing of thin films is the ability to adjust the film properties by changing the process parameters. Relevant process parameters of PECVD are deposition pressure, temperature, reactant gas mixture, and power of the RF field which excites the plasma. Reflection losses of the solar cell are mainly determined by the optical properties of the anti-reflection coating.

The use of thin passivating oxides underneath an ARC reduces the surface recombination velocity (Fossum & Burgess, 1978). Furthermore, these oxides need to be as thin as possible so that the ARC properties of MgF_2/ZnS, SiN, or TiO_2 remain beneficial. On the other hand, reducing the thickness of the oxide below 20 nm reduces the effectiveness of its passivating property (Wang, 1992). In ARC, some researchers such as Qingna *et al*. (2007) who deposited CeO_2-TiO_2/SiO_2 coated on glass substrate, used two layers of anti-reflection and sol-gel method. In their study of inter-diffusion between two layers, a micro structure of mixed layers was formed and distributed in an inclining structure. In the present study, the oxide will be grown with a layer thickness of about 100 nm deposited on the surface, using the conventional furnace at 800°C for 10 minutes.

2.5 Annealing

Neuhaus and Munzer (2007) deposited Ag on the front side and Al on the rear side simultaneously in a furnace. The furnace has several zones that can be heated up to 1000°C separately with IR heaters.

The annealing process was performed to increase the minority carrier diffusion length and to lower the resistivity. Onimisi (2008) has revealed that the annealing process carried out at 500°C for 1.5 hours has the effect of decreasing the resistivity of Cu_2O solar cell samples by nearly 36% compared with the un-annealed samples under the same condition. In ZnO/Al multilayered films, the annealing temperature is the key factor to optimize conducting property (Hu *et al.*, 2006). Li Cai and Ajeet Rohatgi (1997) studied the effect of annealing on the crystalline silicon solar cell and they found an increase in efficiency from 15.8% – to 16.4% at 400°C for 20 minutes. However, the efficiency value decreased from 16.4% to 14.6% when annealing temperature was increased from 400°C to 650°C. In this present study, annealing process will be carried out for 30 minutes at 400°C.

2.6 Metallization process

Burgers (2005) has reported that the rear side of the cells was passivated by a 100 nm wet thermal oxide underneath a layer of 3 μm of aluminum which was evaporated. To improve the passivation of the wet thermal oxide and to improve the contact performance on the rear side and on the front side, the cells were annealed for 10 min at a temperature of about 350°C. The cells were metalized by depositing an aluminum alloy on the rear side. As the wafers get thinner, the rear side of the cell has positive effect on the solar cell's properties. The electronic and optical effects can be realized through the back surface field of the silicon-Al alloy. This is because of the reflectivity properties of the Al metallization (Burgers, 2005). Neuhaus and Munzer (2007)

deposited aluminum on the back surface of the solar cell to get a good light reflectance and to improve the electrical conductivity. They deposited many materials: the patterned aluminum areas were plated with Ni as a diffusion barrier to achieve good contact resistance against Cu. Ni plating was followed by Cu plating and finished by an Ag coating to protect the Cu.

Usually, the metallization contact is deposited on the entire back side of the cells, and as fingers on the front side of the cells. The fingers collect the generated current and the main leads serve to interconnect cells so Zhao *et al*. (1996) designed the emitter contact to further reduce the recombination at the emitter contact area. However, an extra masking step was required to open the contact area. A double exposure masking process was employed to open the contact and then the metal pattern.

2.7 Edge shunt isolation (ESI)

Al Rifai *et al.* (2003) investigated the influence of edge etching procedures on the shunt activity. They used a cold solution of KOH (10-30 %) and deposited the created solution at room temperature on the edge area of the solar cell by using a sponge saturated with KOH. Then the wet edge was heated up locally by using a heating plate kept at (100–140)°C. the results of this experiment before and after shunt isolation in Figure 2.4.

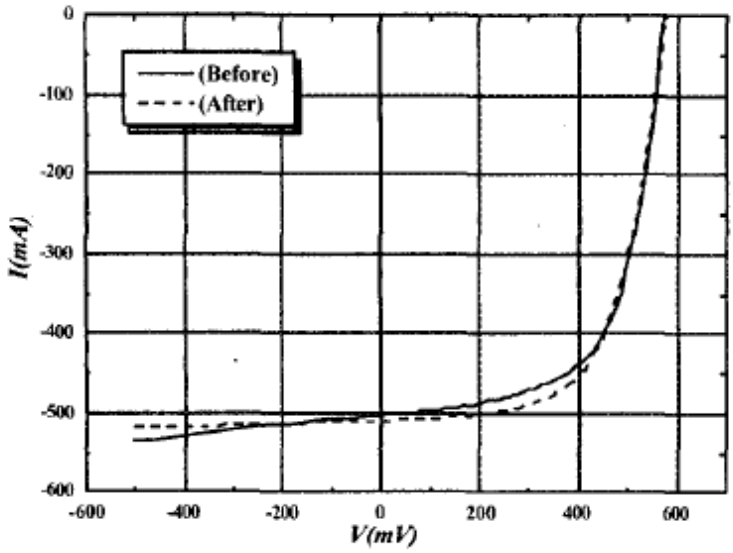

Figure 2.4: The I-V characteristics of the solar cell under illumination before and after the edge passivation [adapted from Al Rifai *et al*., (2003)]

Hamammu and Ibrahim (2002) used a method by making grooves at the cell edge to bypass the emitter; this has lead to an isolation of the shunts at the edge. The main idea is to eliminate the shunts between the emitter and the base. The results obtained before and after the process are shown in Figure 2.5.

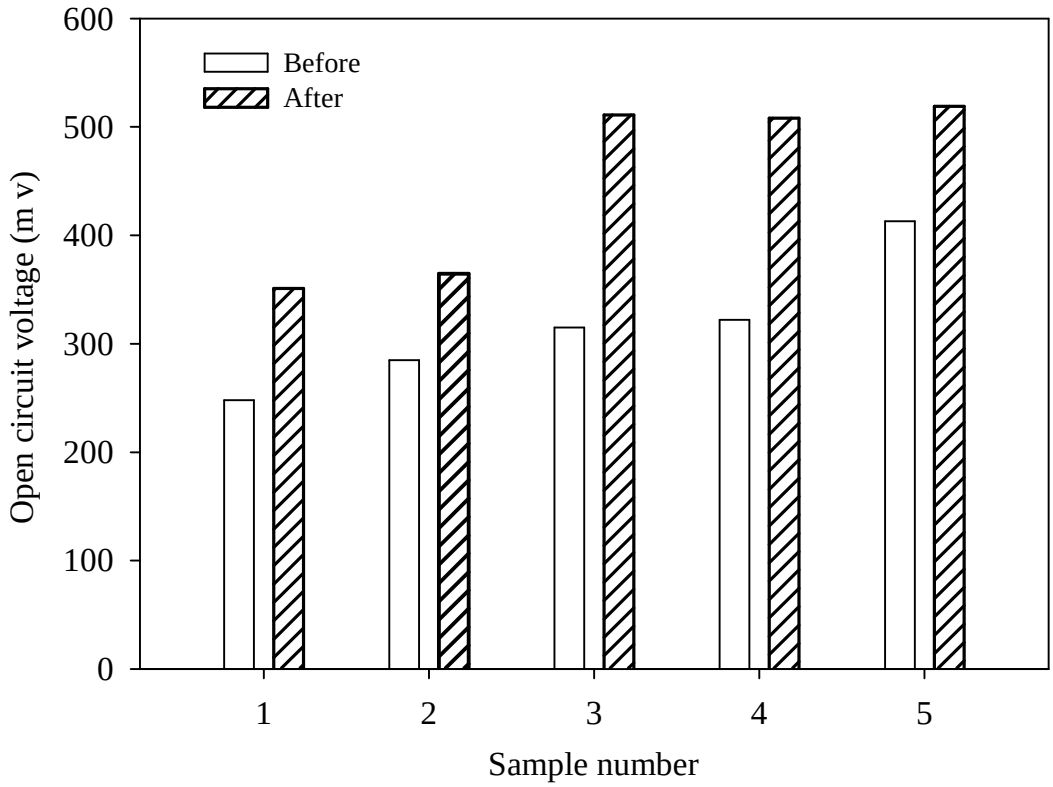

Figure 2.5: The Solar cell open circuit voltage before and after grooving
[Adapted from Hamammu & Ibrahim (2002)]

2.8 Conclusions

After reviewing the literature, the researcher fond that

1- the phosphorus is a potential element that can be used to fabricate the emitter of the solar cell.

2- the boron is also a potential element that can be used to enhance the back surface field which is optimizes the output of the solar cell.

3- the trapping light can be achieved by texturing and anti-reflection coating on the front surface of the solar cell.

4- annealing, metallization, shunt isolation are very important processes as they can be applied to improve the output of the solar cell.

5- Researchers in this area used many parameters to measure the output of solar cells. However, they did not use I_{sc} and V_{oc} independently. This work will use only I_{sc} and V_{oc} because I_{sc} and V_{oc} are main parameters in the solar cell as they can be used to measure the output of the solar cell.

Next chapter will discuss the theoretical concepts of all the processes mentioned above and the mechanism of the solar cell. This is to show how to improve the solar cell.

CHAPTER 3

THE THEORETICAL FRAMEWORK

3.0 Introduction

This chapter explains the principles of how a solar cell is built and its mechanism. Furthermore, the basic equations used in making the solar cell and the excitation for the creation of the p-n junction will be presented first. The mechanism of the solar cell is also presented. A simple measurement of I_{sc} and V_{oc} will be related to the normal I-V characteristics measurement. A number of relevant theoretical concepts for manufacturing the solar cells will also be discussed, such as oxidation and diffusion processes, back surface field, anti-reflection coating, texturing techniques, metallization, and shunt isolation.

3.1 Basic equations

The basic equations are required to consider the current and voltage relationships in the solar cell device. This is to show the relationship between the current density equations and the electric charge in the crystal and the electric field strength. The continuity equation determines the relationship between the generation and recombination of the carriers. Therefore, the three equations are presented below.

3.1.1 Poisson's equation

This equation connects the electric field gradient with the space charge. This comes in one dimension as follows:

$$-\frac{d^2 j}{dx^2} = \frac{dE}{dx} = \frac{r}{ee_o} \tag{3.1}$$

where ϕ is the electric potential, ε is the materials permittivity, and ε_o is the permittivity of the space. Consequently, the electrons in the conduction band represent the negative charge; while the holes in the valence band represent the positive charge. Thus, the Equation 3.1 can be re-written as follows:

$$\frac{dE}{dx} = \frac{q}{ee_O}\left(p - n + N_D^+ - N_A^-\right) \tag{3.2}$$

where n and p are densities of the electrons and the holes respectively; while N_D^+, N_A^- are densities of the ionized donors and acceptors respectively.(Goetzberger *et al*., 1997)

3.1.2 Current density equations

The current of p-n junction contains electrons and holes. The following equations explain the mechanism (i.e. drift and diffusion) of each of them (Sze, 2001).

$$I_n = q\left(n m_n E + D_n \frac{dn}{dx}\right) \tag{3.3}$$

$$I_p = q\left(p m_p E + D_p \frac{dp}{dx}\right) \tag{3.4}$$

where I_n and I_p are the total electrons and holes of the current densities respectively. The first terms ($qn\mu_n E$) and ($qp\mu_P E$) in Equations (3.3 and 3.4) represent the drive current which is driven by the electric field, whereas, the second ($D_n\, d_n/dx$, $D_p\, dp/dx$) terms represent the diffusion current which is driven by the concentration gradient (Sze, 2001).

The mobility $\mu_{p,n}$ and diffusion constants $D_{p,\ n}$ are correlated through Einstein's following equation:

$$D_{n,p} = \frac{k\ T}{q} m_{n,p} \tag{3.5}$$

3.1.3 Continuity equation

Continuity equation explains the relationship between the gradient of the current diffusion to the generation and recombination rates of the charged carriers. These could be given by the formulae 3.6 and 3.7 as follows:

$$\frac{1}{q}\frac{dI_n(x)}{dx} = U - G \tag{3.6}$$

$$\frac{1}{q}\frac{dI_P(x)}{dx} = U - G \tag{3.7}$$

In these formulae, G is the carrier's generation rate and U is the recombination rate of the carriers by the external process, such as illumination (Sze, 2001).

3.2 The principle of solar cells

The creation of the electric current under certain conditions is due to the absorption of light (photons). The principle of transformation is based upon the fact that the un-conducted electrons in semiconductors can be converted into freely moving conducted electrons which simultaneously create holes as second carriers with opposite charges. Since the p-n junction is created in semiconductors, the potential difference exists and forces the charge carriers to travel to the external circuits. The charge carriers have to exist until they reach the barrier potential. Furthermore, the lifetime and diffusion length are key factors for the solar cell

efficiency. The cell design also helps to improve the efficiency (Goetzberger *et al*., 1997).

3.3 The mechanism of solar cells

In order to understand how a solar cell works, it is necessary to understand the p-n junction structure. A p-n junction is formed when the p-type and n-type of the semiconductor materials are brought into contact with each other. The electrons move from n-type to p-type in a diode because of the concentration gradient of the electrons in the n-type. Similarly, the holes move from p-type part to n-type region because of the concentration gradient in the p-type. As a result of the diffusion of current (electron and hole), n-type semiconductor becomes positively charged (donor) and the p-type semiconductor becomes negatively charged (acceptor) in the contact area. As a result, a space charge region is depleted (Goetzberger *et al*., 1997).

.

3.3.1 P-n junction structure

The p-n junction consists of two regions doped differently. The left region is p-type with the acceptor density N_a, and the right region is n-type with the donor density N_d (see Figure 3.1). The dopant must be shallow and the major carriers in both types is approximately equal; while, the concentration of the minor carriers in both types is approximately equal. The basic equations explain the p-n junction behaviour in a solar cell under the influence of the electric field or light. This changes the thermal equilibrium of the p-n junction. These equations are simplified to one dimension, especially in the case of p-n junction. These equations are briefly discussed in Zeghbroeck (2007).

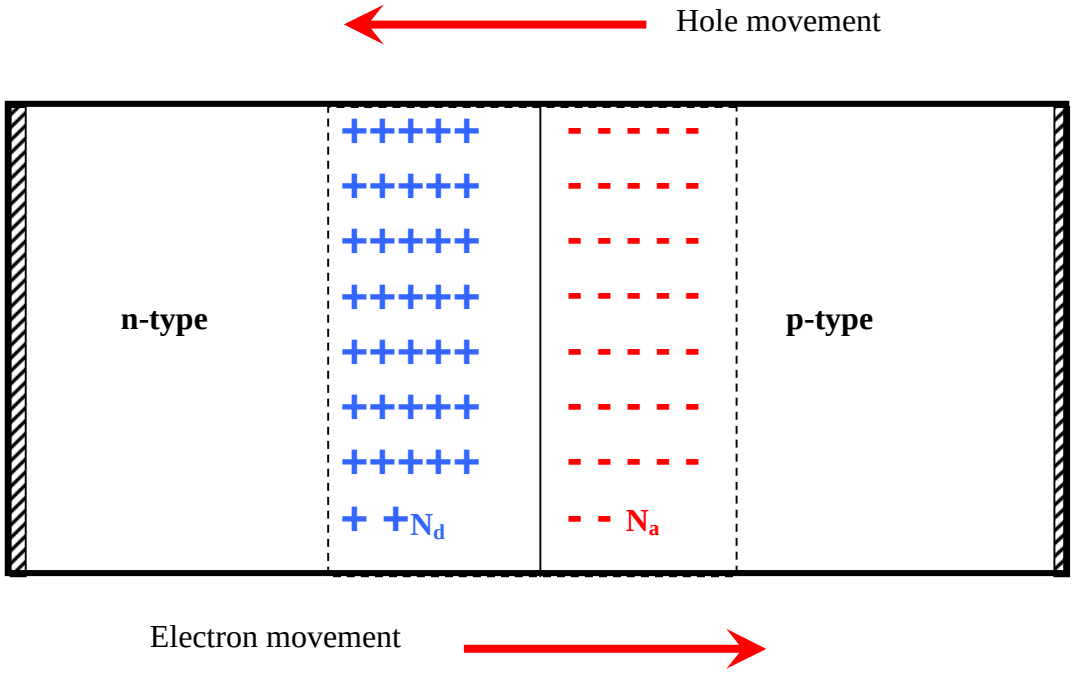

Figure 3.1: Cross-section of p-n junction [adapted from Zeghbroeck, (2007)].

3.3.2 P-n junction in equilibrium

The acceptor and donor create an internal electric field in the depletion region which includes the drift field of minority carriers: holes from n-type and electrons from p-type.

The motion of the electrons and holes increases the diffusion current. Thereafter, the magnitude of the electric field in the junction increases. The p-type has a large concentration of holes and few electrons; the converse is true for n-type. After joining the two regions, the diffusion of the carriers takes place because of the large carrier concentration gradient at the junction. The electrons diffuse from n to p leaving behind the uncompensated donors N_d in the n-type. While, the holes diffused from p to n leave the uncompensated acceptors N_a in the p-type as shown in Figure 3.1. Then, the donors and acceptors create the drift current in the opposite direction to the diffusion current. The carriers in the diffusion current keep moving until the

sum of the diffusion current and the drift current in the junction area equals zero (see Figure 3.2) (Van Overstraeten & Mertens, 1986).

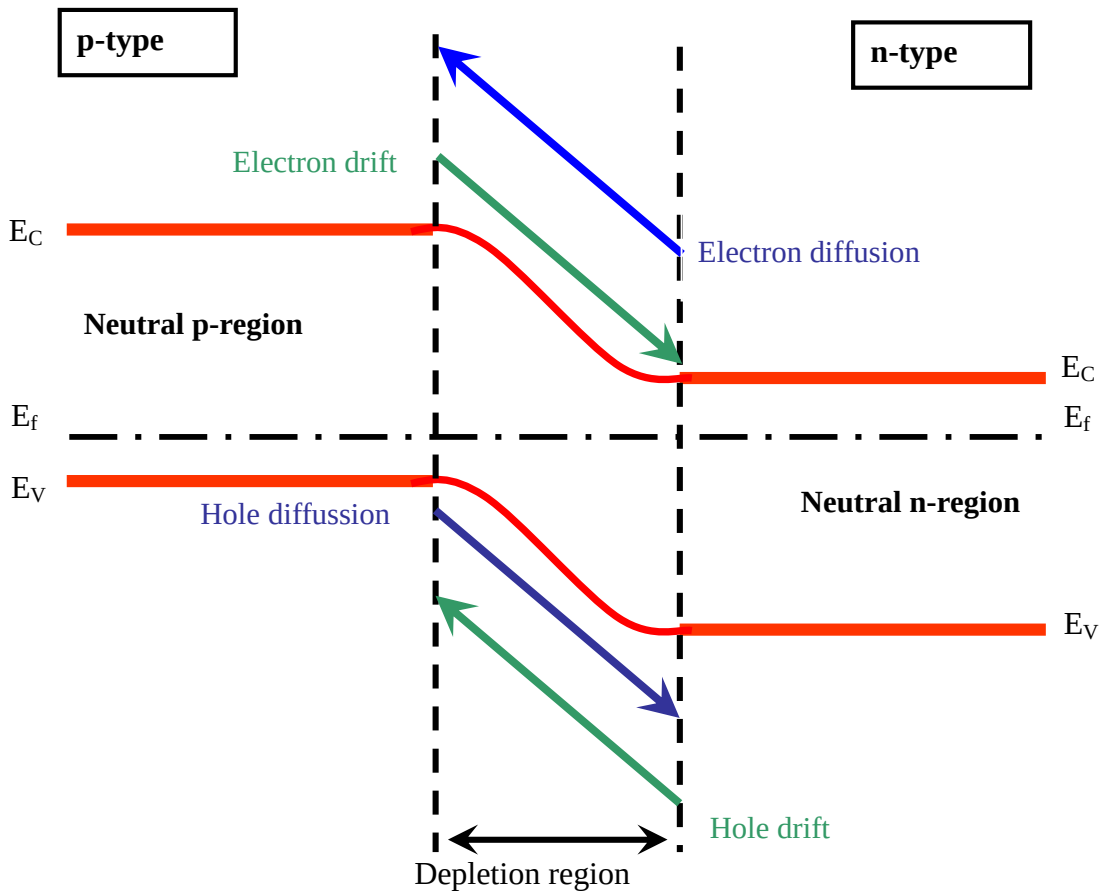

Figure 3.2: The thermal equilibrium currents of p-n junction [adapted from Streetman, (1995)]

When the condition of the current is balanced, the space charge region is in thermal equilibrium. The electric field functions as a barrier to prevent moving more electrons from n-type to p-type, except for the electrons with sufficient energy. The majority of the carriers are dominant carrier types ($n_n >> p_n$ and $p_p >> n_p$); where n_n is